



ELSEVIER

Available online at [www.sciencedirect.com](http://www.sciencedirect.com)

SCIENCE @ DIRECT®

Nuclear Instruments and Methods in Physics Research B 202 (2003) 138–142

**NIM B**  
Beam Interactions  
with Materials & Atoms

[www.elsevier.com/locate/nimb](http://www.elsevier.com/locate/nimb)

## Statistical 3D damage accumulation model for ion implant simulators

J.M. Hernández-Mangas \*, J. Lázaro, L. Enriquez, L. Bailón,  
J. Barbolla, M. Jaraíz

*Departamento de Electricidad y Electrónica, Universidad de Valladolid, E-47011 Valladolid, Spain*

### Abstract

A statistical 3D damage accumulation model, based on the modified Kinchin–Pease formula, for ion implant simulation has been included in our physically based ion implantation code. It has only one fitting parameter for electronic stopping and uses 3D electron density distributions for different types of targets including compound semiconductors. Also, a statistical noise reduction mechanism based on the dose division is used. The model has been adapted to be run under parallel execution in order to speed up the calculation in 3D structures. Sequential ion implantation has been modelled including previous damage profiles. It can also simulate the implantation of molecular and cluster projectiles. Comparisons of simulated doping profiles with experimental SIMS profiles are presented. Also comparisons between simulated amorphization and experimental RBS profiles are shown. An analysis of sequential versus parallel processing is provided.

© 2002 Elsevier Science B.V. All rights reserved.

*PACS:* 34.10.+x; 61.72.Tt; 61.72.–y; 61.82.–d; 61.85.+p; 68.55.Ln

*Keywords:* Ion implantation; Computer simulation; Damage accumulation

### 1. Introduction

Ion implantation is one of the most important methods employed for selective doping of semiconductors. The prediction of impurity distributions obtained in ion implantations is feasible using computer simulation, avoiding expensive experiments. Two methods are, usually, employed to make the simulations: molecular dynamics

(MD) [1] and binary collision approximation (BCA) [2–4], which is faster although less accurate than MD.

Physically based models must be used to simulate the behavior and trajectories of projectiles in a three-dimensional crystalline target structure in order to predict the 3D doping and amorphization profiles. Our simulator includes a physically based model for inelastic stopping that uses only one fitting parameter,  $r_s^0$ , that depends on the ion-target combination [4,5]. It also uses 3D electron density distributions.

This work presents several new features of our BCA ion implant simulator (IIS) that includes a statistical 3D damage model based on the

\* Corresponding author. Tel.: +34-983-423000; fax: +34-983-423675.

*E-mail address:* [jesman@ele.uva.es](mailto:jesman@ele.uva.es) (J.M. Hernández-Mangas).

Kinchin–Pease modified formula [6], an automated statistical noise reduction mechanism based on dose division and a new parallelized scheme to speed up the total calculation time.

**2. Three-dimensional damage accumulation model**

*2.1. Model basis*

The crystalline target is divided into regions as shown in Fig. 1. The front surface of each region has an area,  $A = N_{\text{sim}}/\Phi$ , where  $N_{\text{sim}}$  is the number of simulated ions and  $\Phi$  is the dose. The depth of each region is dynamically adjusted to keep a fixed number of boxes in depth, so as not to increase the computational resources. The damage accumulation process has two stages:

- (a) First, the projectile generates damage along its trajectory. The number of point defects generated,  $n$ , is obtained by means of the modified Kinchin–Pease formula:  $n = kE/(2E_d)$ , where  $E$  is the energy transferred by the projectile to the target atoms in nuclear scattering,  $k = 0.8$  is a constant and  $E_d$  is the displacement energy (e.g. 15 eV for silicon) of the lattice atoms. Only a fraction,  $f_{\text{surv}}$ , of the point defects survives the recombination with other defects, so the net increase of point defects  $\Delta n$  is given by:  $\Delta n = nf_{\text{surv}}(1 - N/N_\alpha)$ , where

$N$  is the previous local defect density of the crystal and  $N_\alpha$ , the local defect density above which the crystal is amorphized (e.g.  $N_\alpha = 10\%$  of the atomic density of silicon [7]). The increase in the number of defects is greater when the crystal is not amorphized than when the crystal is partially amorphized. Finally, the new defect density at each box will be  $N = N + \Delta n/V$ ,  $V$  being the box volume.

- (b) Second, when a projectile enters a partially damaged region, its trajectory depends on the amorphization level of that region. If the local defect density,  $N$ , is near 0 the behavior is like the projectile entering a perfect crystalline target. On the contrary, if  $N$  almost reaches  $N_\alpha$  the behavior is like entering an amorphous target, then a random number is compared with the fraction  $N/N_\alpha$  before performing each scattering event. If the random number exceeds  $N/N_\alpha$ , then the scattering takes place like in a perfect crystalline lattice. Otherwise, the scattering is simulated like in an amorphous target: the crystal lattice is rotated randomly [4], the scattering is performed, and finally the crystal lattice orientation is restored.

The inset in Fig. 2 shows a two-dimensional slice ( $y = 0$ ) of the three-dimensional statistical

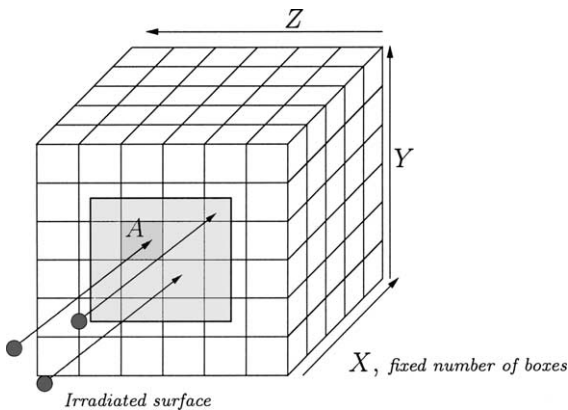


Fig. 1. Three-dimensional scheme of the crystal division into regions. Crystal amorphization is calculated for each region.

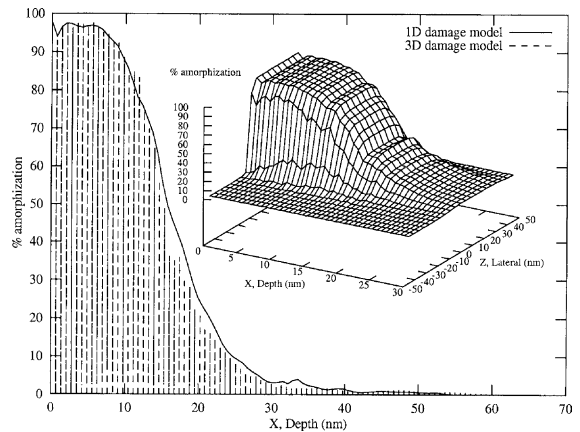


Fig. 2. Comparison between one-dimensional and three-dimensional damage model at line  $y = 0$ ,  $z = 0$ . Inset: two-dimensional slice for  $y = 0$  of the three-dimensional damage.

damage obtained with our new model for an implantation of boron ( $0^\circ$  tilt,  $0^\circ$  rot.) into silicon  $\{100\}$ . The implantation window in the three-dimensional simulation is  $44.7$  by  $44.7$  nm<sup>2</sup> wide and there are not periodic boundary conditions. The damage description is three-dimensional but for illustration purposes we only show a two-dimensional slice. A comparison between three-dimensional projection (line  $y = 0$ ,  $z = 0$ ) and one-dimensional [4] damage model is shown in Fig. 2. They both show the same behavior in the center region of the three-dimensional profile. This means that the three-dimensional model works at least as well as one-dimensional damage model.

In order to avoid the statistical noise in the low concentration doping zones an automatic noise reduction mechanism based on dose division [8] has been developed. The total number of ions simulated is  $M_T$ . We simulate  $m$  stages of  $M$  ions ( $M_T = mM$ ). At each stage, each simulated ion represents a different dose fraction. The first  $M$  ions represent a very low dose fraction (e.g.  $10^{12}$  at/cm<sup>2</sup>). We achieve statistical accuracy in the lower concentration doping zone of the final profile due to the low damage generated and the channelling phenomena. Next  $M$  ions represent a higher dose fraction (e.g. 10 times more than the previous one) and they are implanted taking into account the previous damage. We obtain statistical accuracy in the middle concentration zones of the final profile due to a higher damage and a lower channelling

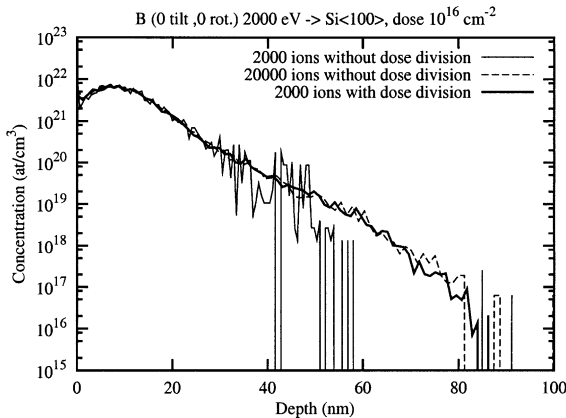


Fig. 3. Simulated doping profiles using and not using the dose division algorithm.

Table 1

Time simulation comparison using and not using the dose division algorithm

Energy (eV)	Time (s)		Time (s)
	2000 Ions	20,000 Ions	2000 Ion with dose division
2000	46.5 ( $\times 1$ )	631 ( $\times 13.4$ )	205 ( $\times 4.3$ )
20,000	265 ( $\times 1$ )	3163 ( $\times 11.9$ )	1116 ( $\times 4.2$ )
200,000	1424 ( $\times 1$ )	14,253 ( $\times 10.0$ )	4648 ( $\times 3.2$ )

phenomena. Finally, last  $M$  ions represent the remainder dose fraction. With this algorithm, we describe with enough statistical accuracy the whole doping concentration range of the final profile. Fig. 3 shows a comparison of simulated profiles using and not using the noise reduction algorithm. To achieve enough statistical accuracy in the tail of the impurity profile of a high dose implant we need to simulate 20,000 ions. Only 1/3 calculation time (see Table 1) is needed when using the dose division algorithm ( $m = 4$  stages and  $M = 2000$  ions) to achieve similar statistical accuracy.

## 2.2. Model parallelization

Three-dimensional damage accumulation modelization is very time and resources consuming. In order to speed up the simulations a parallelized version of the IIS code, that runs in a heterogeneous workstation cluster, has been developed. We use the PVM library [9] using a master–slave configuration. Master process distributes work among slave processes. Each slave simulates one projectile's cascade and returns data about damage and projectile's position to the master process. The slave processes do not see the damage produced by other concurrent cascades to prevent communication network overload. We need to know the incremental damage produced by each slave process in order to be accumulated by the master process because the damage accumulation is not linear. Then, the master will propagate the new defect density among the slave processes.

The master process, after the  $i$ th cascade, accumulates total damage using the equation  $N_i[\ ] = N_{i-1}[\ ]A[\ ] + B[\ ]$  where  $N_i[x, y, z]$  is the updated defect density for each box and  $A[x, y, z]$

and  $B[x, y, z]$  are two 3D arrays that include the incremental damage information generated by the slave. Initially,  $A_0[\ ] = 1$  and  $B_0[\ ] = 0$ . These arrays are updated after each collision (index  $j$ ) following the equations  $A_j[\ ] = A_{j-1}[\ ](1 - (n_j f_{\text{surv}} / N_\alpha V))$  and  $B_j[\ ] = B_{j-1}[\ ](1 - (n_j f_{\text{surv}} / N_\alpha V)) + (n_j f_{\text{surv}} / V)$  that have been obtained from the basic model (see Section 2.1). Each slave process, at the end of a cascade simulation, sends final  $A[\ ]$  and  $B[\ ]$  arrays to the master to update the total damage that will be taken into account in subsequent cascades.

The simulator throughput is practically multiplied by the number of slaves. However, a weak saturation is observed when the number of slaves grows, due to data transfers between processes.

### 3. Experimental validation

Fig. 4 shows the comparison between simulated and experimental SIMS [8] impurity profiles for an implantation of boron into silicon {100} with energies of 15, 35 and 80 keV, dose of  $5 \times 10^{14}$  at/cm<sup>2</sup> and 1° tilt and 0° rotation. We use only one fitting parameter,  $r_s^0 = 1.85$ , for electronic stopping and,  $f_{\text{surv}} = 0.06$  and  $N_\alpha = 4.99 \times 10^{21}$  at/cm<sup>3</sup> for the 3D damage accumulation model. The agreement with experimental profiles is excellent.

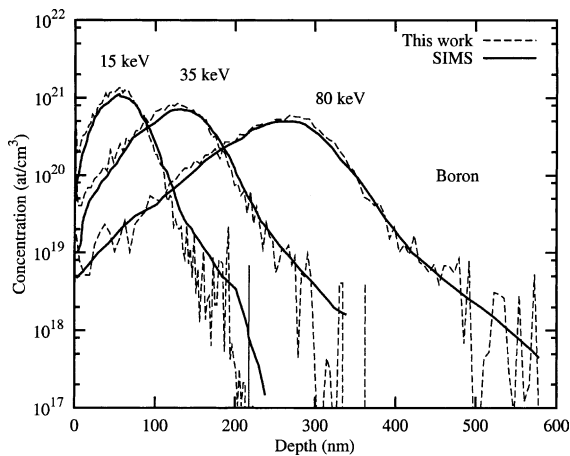


Fig. 4. Simulated and experimental SIMS [12] impurity profiles corresponding to boron (1°, 0°) into silicon {100} implantation. Energies are 15, 35, 80 keV, dose is  $8 \times 10^{15}$  at/cm<sup>2</sup>.

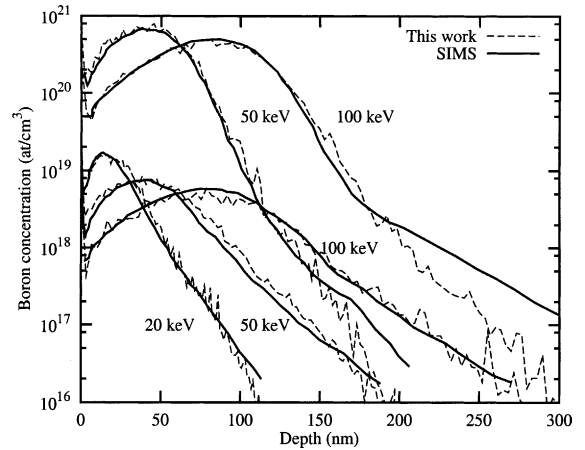


Fig. 5. Multiple implant of  $\text{BF}_2$  projectile with several energies and orientations: 20, 50, 100 keV (7°, 22°), with  $5 \times 10^{13}$  at/cm<sup>2</sup>; 50, 100 keV (7°, 0°) with  $4 \times 10^{15}$  at/cm<sup>2</sup>. Comparison with experimental SIMS profiles [10] is presented. The agreement is good enough.

An example of molecular implantation is shown in Fig. 5. It shows the impurity profiles for a wide range of  $\text{BF}_2$  implantations into silicon {100}; energies of 20, 50 and 100 keV, doses of  $5 \times 10^{13}$  and  $4 \times 10^{15}$  at/cm<sup>2</sup>, and several crystal orientations (7°, 22°) and (7°, 0°). The agreement between simulated and experimental SIMS [10] profiles is excellent for, at least, three orders of magnitude.

Comparison between SIMS experimental results and simulated impurity profiles for arsenic (1°, 0°) into silicon {100} implants with 50 and 100 keV with doses of  $10^{14}$  and  $5 \times 10^{14}$  at/cm<sup>2</sup>, respectively are shown in Fig. 6 (top). In general the agreement is good enough. A comparison with RBS experimental damage profiles are also shown in Fig. 6 (bottom). In these cases we use a value of 2.00 for  $r_s^0$  and  $f_{\text{surv}} = 0.40$  and  $N_\alpha = 4.99 \times 10^{21}$  at/cm<sup>3</sup>. The main features of the experimental profiles are given by the simulated profiles in this case.

### 4. Conclusions

The simulation results obtained with the presented 3D model match well with the results provided by the previous one-dimensional model. This 3D model has been validated by means of a

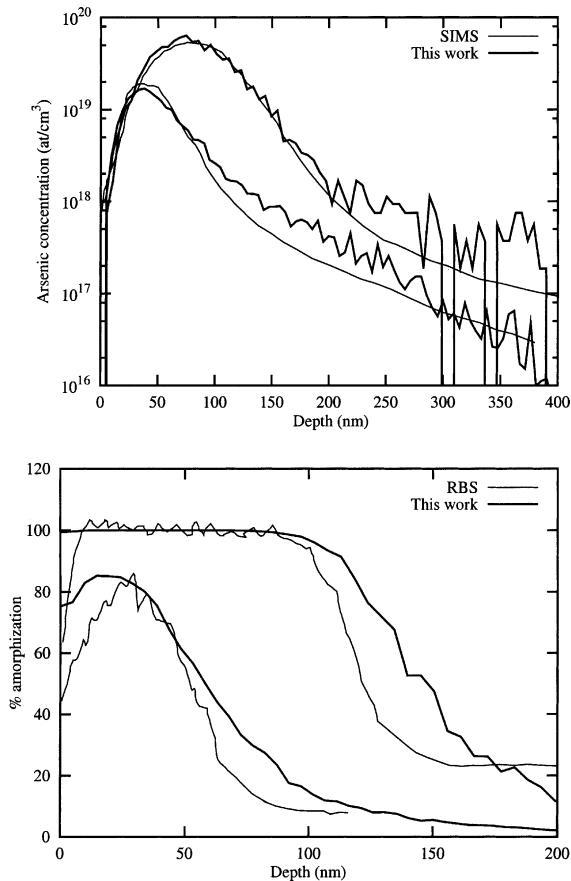


Fig. 6. Comparison of simulated and experimental SIMS (top) and RBS (bottom) profiles [8] for arsenic ( $1^\circ, 0^\circ$ ) into silicon  $\{100\}$  with energies and doses of 50 keV,  $10^{14}$  at/cm $^2$  and 100 keV,  $5 \times 10^{14}$  at/cm $^2$ , respectively.

comparison set between simulated and experimental results covering several projectiles and implant conditions. Two methods are suggested to speed up the calculation time: a parallelized algo-

rithm and an automatic dose division algorithm. Another method could be a trajectory replication mechanism as proposed by Li et al. [11].

### Acknowledgements

This work was performed under the auspices of the Junta de Castilla y León (VA 14/00B) and the DGICYT project no. PB 98-0398.

### References

- [1] K. Beardmore, N. Gronbeck-Jensen, Phys. Rev. E 57 (6) (1998) 7278.
- [2] K. Klein, C. Park, A. Tasch, IEEE Trans. Elect. Dev. 39 (7) (1992) 1614.
- [3] D. Cai, N. Gronbeck-Jensen, C. Snell, K. Beardmore, Phys. Rev. B 54 (23) (1996) 17147.
- [4] J. Hernández-Mangas, J. Arias, M. Jaraíz, L. Bailón, J. Barbolla, J. Appl. Phys. 91 (2) (2002) 658.
- [5] J. Hernández-Mangas, L. Enriquez, J. Arias, M. Jaraíz, L. Bailón, Solid State Electron. 46 (2002) 1315.
- [6] G. Kinchin, R. Pease, Rep. Prog. Phys. 18 (1955) 1.
- [7] G. Wang, S. Tian, M. Morris, B. Obradovich, G. Balamurugan, A. Tasch, Microelectronic Device Technology, Austin, TX, USA, SPIE-Int., Soc. Opt. Eng. (1997) 324.
- [8] T. University of Austin, UT-MARLOWE 5.0 User's guide., <http://homer.mer.utexas.edu/TCAD/utmarlowe>, 1999.
- [9] J. Dongarra, A. Geist, R. Mancheck, V. Sunderman, Comput. Phys. 7 (2) (1993) 166.
- [10] A. Hössinger, S. Selberherr, M. Kimura, I. Nomachi, S. Kusanagi, Electrochem. Soc. Proc. 99-2 (1999) 18.
- [11] D. Li, G. Wang, Y. Chen, L. Lin, G. Shrivastav, S. Oak, A. Tasch, S. Banerjee, S. Obradovich, Nucl. Instr. and Meth. B 184 (2001) 500.
- [12] A. Hössinger, S. Selberherr, in: Proceedings of 2nd International Conference on Modeling and Simulation of Microsystems, 1999.